

Interplay of dynamical and equilibrium phenomena in vortex matter

This article has been downloaded from IOPscience. Please scroll down to see the full text article.

2002 J. Phys.: Condens. Matter 14 2403

(<http://iopscience.iop.org/0953-8984/14/9/329>)

View [the table of contents for this issue](#), or go to the [journal homepage](#) for more

Download details:

IP Address: 171.66.16.27

The article was downloaded on 17/05/2010 at 06:17

Please note that [terms and conditions apply](#).

Interplay of dynamical and equilibrium phenomena in vortex matter

Mario Nicodemi

Università di Napoli ‘Federico II’, Dipartimento Scienze Fisiche, INFN and INFN, Via Cintia, 80126 Napoli, Italy

E-mail: mario.nicodemi@na.infn.it

Received 22 November 2001

Published 22 February 2002

Online at stacks.iop.org/JPhysCM/14/2403

Abstract

We review the role of dynamical effects and the important interplay of off-equilibrium and equilibrium phenomena in the physics of magnetic and transport properties of vortex matter in type-II superconductors. More specifically, we discuss the unifying framework of these phenomena emerging in the context of a recently introduced model for vortices and their important deep relations with other glass formers.

(Some figures in this article are in colour only in the electronic version)

1. Introduction

The existence of ‘aging’ phenomena in vortex matter of type-II superconductors has long been a subject of debate [1]. Interestingly, new discoveries [2–5] have clearly shown the presence of this kind of phenomenon in vortex physics. ‘Aging’ and ‘memory’ have been observed for instance in vortex magnetic creep [2, 3] (i.e., in the relaxation of vortex density) as well as in transport properties (i.e., in presence of an applied current), where ‘irreversible’ I – V characteristics have been found along with history-dependent critical current and many other similar effects [4, 5]. Interestingly, these experiments show a very broad agreement with theoretical predictions from a recently introduced vortex model [6] and these results are changing the scenario of our understanding of several issues in the physics of vortices. In the present paper we briefly review this topic in the framework of the schematic model of [6] and, more specifically, we discuss dynamical phenomena and their relations to the underlying equilibrium properties of vortex matter. In particular, we will discuss the non-equilibrium effects observed in magnetization hysteresis loops and the associated phase transitions. In order to give a unifying picture, we also analyse the relations to history-dependent effects in I – V characteristics. The connections with other ‘glassy’ systems, such as glass formers and spin glasses [7], are also briefly outlined.

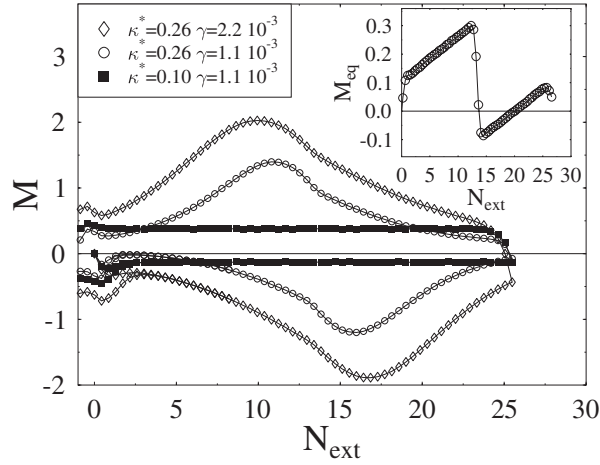


Figure 1. Main panel: the magnetization, M , as a function of the applied field density, N_{ext} , in the ROM at $T = 0.3$ for the sweep rates γ and κ^* shown. Notice the appearance of a ‘second magnetization peak’ when κ^* is large enough. Inset: the equilibrium value of M (i.e., when the field ramp rate $\gamma \rightarrow 0$) at $T = 0.3$ ($\kappa^* = 0.26$).

2. The restricted occupancy model (ROM)

For sake of clarity we briefly recall the properties of the vortex model that we introduced in [6]: let us consider a system of straight parallel vortex lines, corresponding to a magnetic field B along the z -axis. The typical high vortex densities and long field penetration length, λ , imply that each vortex is strongly interacting with very many others, resulting in there being a formidable technical problem to be solved. The approximation proposed in [6] consists in coarse graining the system in the xy -plane by introducing a square grid of lattice spacing, l_0 , of the order of the London length, λ . The number of vortices on the i th coarse-grained cell, n_i , is an integer smaller than $N_{c2} = B_{c2}l_0^2/\phi_0$ (B_{c2} is the upper critical field and $\phi_0 = hc/2e$ is the flux quantum). The coarse-grained interaction Hamiltonian is thus [6]: $\mathcal{H} = \frac{1}{2} \sum_{ij} n_i A_{ij} n_j - \frac{1}{2} \sum_i A_{ii} |n_i| - \sum_i A_i^p |n_i|$. The first two terms describe the repulsion between the vortices and their self-energy, and the last the interaction with a random pinning background. For the sake of simplicity, we consider the simplest version of \mathcal{H} : we choose $A_{ii} = A_0 = 1$; $A_{ij} = A_1 < A_0$ if i and j are nearest neighbours; $A_{ij} = 0$ otherwise; the random pinning is delta-distributed around zero and a value A_0^p —it is given by¹ $P(A^p) = (1 - p)\delta(A^p) + p\delta(A^p - A_0^p)$. Particles have a ‘charge’ $s_i = \pm 1$ corresponding to opposite directions of magnetic flux (i.e., $n_i \rightarrow s_i n_i$) and neighbouring particles with opposite ‘charge’ annihilate. In analogy with computer investigations of dynamical processes in fluids, the time evolution of the model is simulated by a Monte Carlo Kawasaki dynamics on a square lattice of size L at a temperature T (see footnote 1 again). The system is periodic in the y -direction. The two edges parallel to the y -axis are in contact with a vortex reservoir, i.e., an external magnetic field, of density N_{ext} . Particles can enter and leave the system only through the reservoir. The above ROM is described in [6].

¹ Here $A_0^p = 0.3A_0$, $N_{c2} = 27$, $p = 1/2$ and, with the notation used here, $A_1 = 0.28A_0$ (the \mathcal{H} -parameters can be related to the real material parameters [6]). L is taken up to $L = 128$.

3. Magnetic properties

In this section, we are going to discuss the dynamical behaviour of the magnetization of the ROM and its relation to the equilibrium phase transition. In our Monte Carlo simulations the system is prepared by zero-field cooling and then increasing N_{ext} at a constant rate, γ , up to a given value and then decreasing it back to zero at the same rate. At this point, we have no externally applied currents. In particular, we record the magnetization as a function of N_{ext} :

$$M(t) = N_{\text{in}}(t) - N_{\text{ext}}(t) \quad (1)$$

where $N_{\text{in}} = \sum_i n_i / L^d$ is the number of particles inside the system and the Monte Carlo time, t , is measured in units of single attempted updates per degree of freedom. In agreement with experiments [8], at low temperatures pronounced hysteretic magnetization loops are seen when M is plotted as a function of N_{ext} [6] (see figure 1). Furthermore, when κ^* is larger than a critical value $\kappa_c^* \simeq 0.25$ —as large as in experiments on superconductors (see [1, 8])—a definite *second peak* appears in $M(N_{\text{ext}})$ [6]. Such a second peak (called ‘anomalous’, because it is at odds with previous scenarios of vortex physics) is related to a new phase transition in the vortex system observed at moderately high applied fields, as we explain below.

The actual shape of the loops depends on the system parameters and, in particular, on the rate of sweep of the external field, γ , as shown in figure 1. As soon as the inverse of the sweep rate is smaller than the system characteristic relaxation time (see below), strong hysteresis effects appear. Although the second peak does depend on the dynamics through γ , in the ROM it is related to a new phase transition: in the $\gamma \rightarrow 0$ limit, its location, N_{sp} , is associated with a sharp jump in $M_{\text{eq}} \equiv \lim_{\gamma \rightarrow 0} M(\gamma)$ (see the inset of figure 1). These findings describe very well the known experiments (for instance, see [6, 8] and references therein): in agreement with experiments, our numerical simulations show, on increasing the field (see the inset of figure 1), re-entrant discontinuous transitions at very small and high fields and, between them, another discontinuous transition associated with the location of the second magnetization peak [6].

Our model also explains why around the second peak ‘slushy’ regions have often been observed: the system relaxation time, $\tau_M(N_{\text{ext}})$, has a broad maximum around the second peak (see figure 2), and thus off-equilibrium ‘glassy’ dynamical features appear whenever the system is observed on too-short timescales [6]. Actually, on lowering the temperature, $\tau_M(T)$ shows a steep increase (see figure 3). In fact, for temperatures below $T_g \simeq 0.25$, the characteristic time becomes larger than our recording window and the system definitely loses contact with equilibrium. The crossover temperature $T_g(N_{\text{ext}})$ has a physical meaning similar to the phenomenological definition of the so-called glass transition point in supercooled liquids [7]. The presence of an underlying ‘ideal’ glass transition point, $T_c(N_{\text{ext}})$, can be located by some fit of τ from the high- T regime, such as a Vogel–Tammann–Fulcher law or a power law (see figure 3):

$$\tau = \tau_0 \exp\left(\frac{E_0}{T - T_c}\right). \quad (2)$$

The Vogel–Tammann–Fulcher law has been experimentally observed (see for instance [12]). Below T_g , relaxation times are huge and the system off-equilibrium dynamics has remarkably rich ‘aging’ properties [6].

3.1. Vortex mean square displacement

The microscopic origin of the above features in the system dynamics can be understood by considering the vortex mean square displacement, $R^2(t)$. At high enough T , $R^2(t)$ is linear in t ;

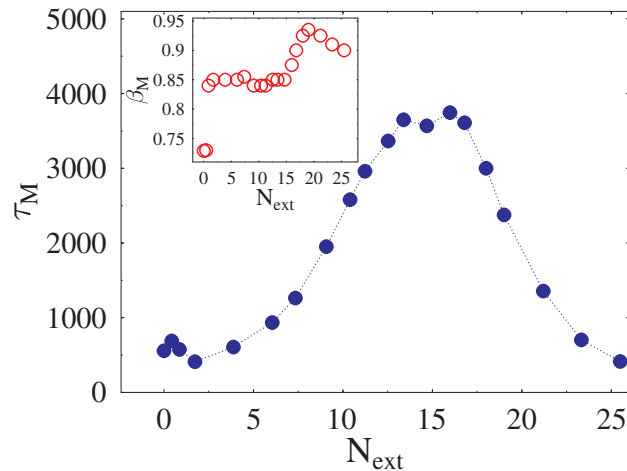


Figure 2. The characteristic time, τ_M , and the Kohlrausch–Williams–Watts exponent, β_M , of the asymptotic magnetic relaxation (here at $T = 1.0$). Inset: β_M as a function of the applied field N_{ext} . Main panel: τ_M as a function of N_{ext} . Notice that τ_M is a non-monotonic function of N_{ext} which spans about one decade. The location of the maximum of τ_M corresponds to the position of the ‘second peak’ observed in magnetization loops (see figure 1). The first peak in τ_M is related to the crossing of the low-field order–disorder transition.

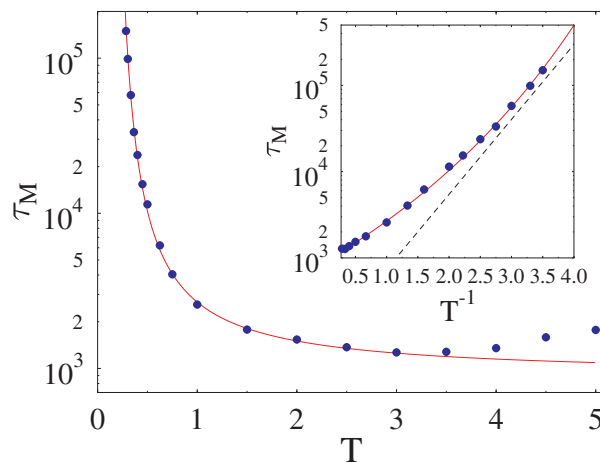


Figure 3. The characteristic time, τ_M , and the Kohlrausch–Williams–Watts exponent, β_M , of the asymptotic magnetic relaxation (here at $T = 1.0$) as a function of the temperature T , recorded at $N_{\text{ext}} = 10$ after ramping the field at a rate γ as in figure 2. The equilibration time τ_M grows enormously on decreasing the temperature T . Below the crossover temperature $T_g \sim 0.25$, the system relaxation times are larger than the observation time. The Vogel–Tammann–Fulcher fit of equation (2) is the superimposed curve. Inset: in the region where τ_M seems to diverge, we plot it as a function of $1/T$ and show the VTF fit of equation (2). For comparison, an Arrhenius curve is also shown (dashed straight line).

but at lower temperatures, typically below T_g , the process becomes asymptotically strongly sub-diffusive: $R^2(t) \simeq Dt^\nu$ with $\nu \ll 1$ (in figure 4, we show D and ν as functions of T). From this point of view, T_g is the location of a sort of structural arrest of the system, where particle displacement is dramatically suppressed. Each vortex is caged by other neighbouring vortices

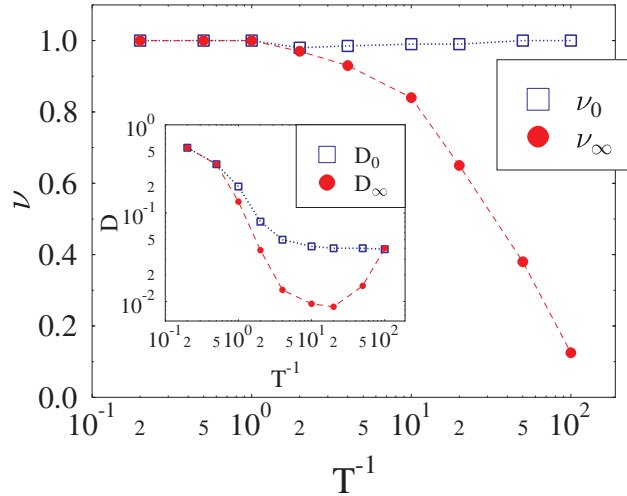


Figure 4. The short-times (asymptotic) diffusion exponent ν_0 (ν_∞) and coefficient D_0 (D_∞) of the mean square displacement, $R^2(t) \simeq Dt^\nu$, as a function of the temperature (at $N_{\text{ext}} = 10$). Below $T_g \simeq 0.25$ the asymptotic dynamics is strongly sub-diffusive ($\nu_\infty \ll 1$).

for long times. The system dynamics needs large-scale ‘cooperative rearrangements’ to relax [7]. Interestingly, a very similar scenario has been recorded in real superconductors [11].

3.2. Anomalous creep at very low temperatures

We can now simply explain another intriguing experimental observation [10] for vortex matter: even at very low temperatures (where activated processes should be absent), magnetic relaxation does take place. This phenomenon, previously interpreted in terms of ‘quantum tunnelling’ of vortices [1], is also found in the present purely ‘classical’ vortex model, where a non-zero creep rate for $T \rightarrow 0$ is just a consequence of the off-equilibrium nature of the low- T dynamics. In the experiments, the dependence of the creep rate, S_a , on T is investigated, where $S_a = |\partial \ln(M)/\partial \ln(t)|$. When $T \rightarrow 0$, in both experiments and in our simulations, S_a approaches a *finite* value, $S_a(0) > 0$ (see figure 5).

We have seen that at very low T , the system equilibration time $\tau(T)$ diverges exponentially. In that region, the typical observation time windows, t_{obs} , are such that $t_{\text{obs}}/\tau \ll 1$, and the system is in the early stage of its off-equilibrium relaxation from its initial state. This is schematically the origin of the flattening of S_a at very low T [6]. In the slow off-equilibrium relaxation at very low temperatures, no activation over barriers occurs and the system simply wanders in its very-high-dimensional phase space through the few channels where no energy increase is required. Experimentally, the present scenario, where off-equilibrium phenomena dominate the anomalous low- T creep, is supported by the discovery of ‘aging’ [2, 4, 8].

4. Vortex flow and I – V characteristics

An external current activates a Lorentz-driven vortex flow in type II superconductors and strong memory and history-dependent effects also appear in the transport (i.e., I – V) properties. In connection with the previous results on magnetic creep, we now discuss such phenomena in I – V characteristics.

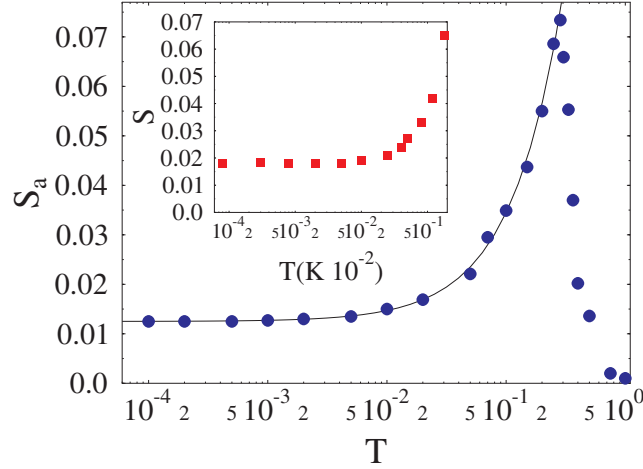


Figure 5. Main panel: the creep rate, S_a , in the ROM ($\kappa^* = 0.28$, $\gamma = 10^{-3}$) for $N_{\text{ext}} = 10$ as a function of the temperature, T , in units of A_0 . The error bars are of the size of the symbols. The superimposed line is a linear fit. Inset: the creep rate measured in BSCCO single crystal by Aupke *et al* [10] for an external field of 880 Oe.

For a given applied field, N_{ext} (below $N_{\text{ext}} = 10$), we monitor the system relaxation in the presence of a drive, I (due to the Lorentz force), in the y -direction. As in similar driven lattice gases [9], the effect of the drive is simulated by introducing a bias in the Metropolis coupling of the system to the thermal bath: a particle can jump to a neighbouring site with a probability $\min\{1, \exp[-(\Delta\mathcal{H} - \epsilon I)/T]\}$. Here, $\Delta\mathcal{H}$ is the change in \mathcal{H} after the jump and $\epsilon = \pm 1$ for a particle trying to hop along or against the direction of the drive, and $\epsilon = 0$ in orthogonal jumps. A drive I generates a voltage V [13]: $V(t) = \langle v_a(t) \rangle$, where $v_a(t) = \bar{v}(t)$ is an average vortex ‘velocity’ at time t [6]. Here, $v(t) = (1/L) \sum_i v_i(t)$ is the instantaneous flow ‘velocity’: $v_i(t) = \pm 1$ if the vortex i at time t moves along the direction of the drive I or in the opposite direction, and $v_i = 0$ otherwise.

4.1. Memory and irreversibility in driven vortex flow

The first interesting manifestation of ‘irreversibility’ and ‘memory’ in the ROM is shown in figure 6. The I – V characteristic is measured by ramping I up to some value I_{max} (see the inset of figure 6). Then I is ramped back to zero, but at a given value I_w the system is allowed to evolve for a time t_w ; finally, I is ramped up again. The resulting *irreversible* $V(I)$ is shown in figure 6. For $I > I_w$ the decreasing branch of the plot (empty circles) slightly deviates from the increasing one (filled circles), showing the appearance of *irreversibility*. This is even more apparent after t_w : for $I < I_w$ the two paths are clearly different. Interestingly, upon increasing I again (filled triangles), $V(I)$ matches not the first increasing branch, but the later, decreasing one: in this sense there is coexistence of memory and irreversibility. Also very interesting is that on repeating the cycle with a new I_w (squares), the system approximately follows the *same* branches. This non-reversible behaviour is also found in other glassy systems [14] The interplay between irreversibility and memory discussed here can be experimentally checked in superconductors and the present scenario assessed.

4.2. History-dependent I – V characteristics

We now discuss another striking manifestation of memory phenomena in the I – V characteristic. As in real experiments on vortex matter [4], we let the system undergo a

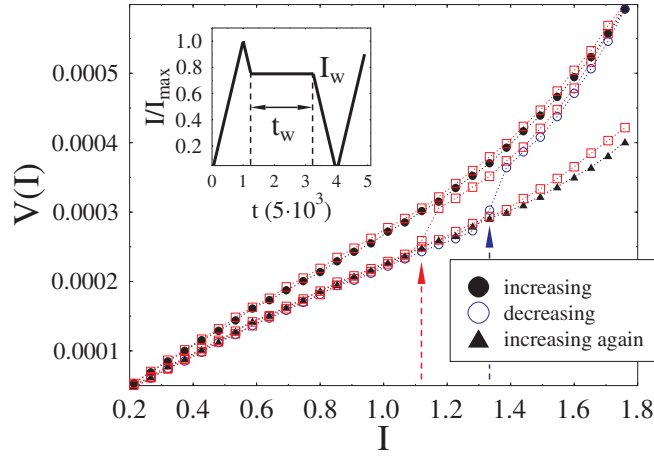


Figure 6. The I - V characteristic is measured at $T = 0.1$ during cycles of I (see also the inset): I is at first increased up to I_{\max} (filled circles); along the descending branch of the cycle (empty circles), when $I = I_w$ (in the main panel $I_w = 3/4I_{\max}$ is indicated by the arrow on the right) the drive is kept fixed for a time $t_w = 10^4$ and then the cycle restarted; finally, I is ramped up again (filled triangles). For $I > I_w$, the first increasing ramp and the decreasing one (respectively filled and empty circles) do not completely match, showing *irreversibility* in the I - V characteristic. After waiting for a time t_w at I_w , a much larger separation is seen. However, on raising I again (filled triangles) a strong *memory* is observed: the system follows not the first branch (filled circles), but the decreasing one (empty circles). Furthermore, in a new cycle (squares) with a lower I_w ($I_w = 2/3I_{\max}$, left arrow), the *same* branches are found.

current step of height I_0 for a time t_0 before starting to record the I - V characteristic while ramping I , as sketched in the inset of figure 7. Figure 7 shows (for $T = 0.1$) that the I - V characteristic depends on the waiting time t_0 . The system response is ‘aging’: the longer t_0 the smaller the response, a phenomenon known as ‘stiffening’ in glass formers [7, 14]. The model also reproduces the experimentally found time dependence of the critical current [4]. Usually, one defines an effective critical current, I_c^{eff} , as the point where V becomes larger than a given threshold (say $V_{\text{thr}} = 10^{-5}$ in our case): one then finds that I_c^{eff} is t_0 - and I_0 -dependent (like in experiments [4], I_c^{eff} is slowly increasing with t_0 ; see figure 7).

In our model we can easily identify the characteristic timescales of the driven dynamics. After applying a drive, I , the system response, V , relaxes following a pattern with two very different parts: at first a rapidly changing non-linear response is seen, which is later followed by a very slow decrease towards stationarity. In agreement with experimental findings [4], the latter has a characteristic double-step structure, which asymptotically can be well fitted by stretched exponentials²: $V(t) \propto \exp(-t/\tau_V)^\beta$. The above long-time fit defines the characteristic asymptotic scale, τ_V , of the relaxation. The exponents β and τ_V are functions of I , T and N_{ext} ; in particular, $\tau_V(I)$ decreases with I and seems to approach a *finite plateau* for $I < I^*$, with $I^* \simeq O(1)$. In this sense, the presence of a drive I makes the approach to stationarity faster and has an effect similar to that of an increase in T .

The above properties of τ_V are sufficient to explain the history-dependent effects found in the experiments previously considered. For instance, the ‘imperfect memory’, discussed above, is caused by the presence of a long, but finite, scale τ_V in the problem: for a given I_1 the system seems to be frozen whenever it is observed on timescales smaller than $\tau_V(I_1)$. Thus, if t_2 is short enough ($t_2 < \tau_V(I_1)$), the system preserves a strong ‘memory’ of its state at t_1 .

² At lower T , inverse logarithmic relaxations are found [6].

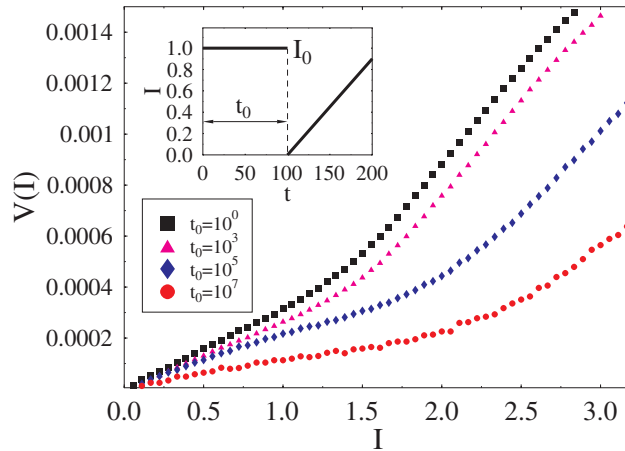


Figure 7. The I - V characteristic obtained at $T = 0.1$ by ramping I after keeping the system in presence of a drive $I_0 = 1$ for a time t_0 as shown in the inset. The response, V , is ‘aging’ (i.e., depends on t_0) and, more specifically, *stiffening*: the longer t_0 , the smaller it is.

The weakening of such a ‘memory’ found for higher currents I_1 (see [6]) is also a consequence of the strong decrease of $\tau_V(I)$ with I . The phenomenon of ‘rejuvenation’ (see [6]) is, in turn, a consequence of the presence of the extremely fast first part of the relaxation found in $V(t)$ upon applying a drive and of the above long-term memory. The existence of the slow part in the $V(t)$ relaxation also affects the ‘stiffening’ of the response in the I - V characteristic of figure 7, which is due to the non-stationarity of the vortex flow on scales smaller than τ_V . Actually, in figure 7, for a given I the value of V on the different curves corresponds to the system being probed at different stages of its non-stationary evolution.

The origin of these time-dependent properties of the driven flow, and in turn those of the I - V characteristics, can be traced back to the concurrent vortex creep and reorganization of vortex domains. In fact, either with or without an external drive, the system evolves in the presence of a non-uniform density profile which in turn relaxes as we discussed in the paragraphs above. An important discovery is that the characteristic times of the voltage and magnetic relaxation are approximately proportional: $\tau_V \propto \tau_M$ [6]. This outlines why the non-stationary voltage relaxation is structurally related to the reorganization of vortices during the creep (a fact confirmed by recent experiments [8]).

4.3. The peak effect in the critical current

Finally, we discuss another important phenomenon discovered in vortex physics [15]: the so-called peak effect (PE) observed in the system critical current, I_c (as in experiments, I_c is defined as the point where the voltage becomes larger than a given threshold, here $V_{\text{thr}} = 10^{-5}$). This surprising effect consists in a non-monotonic behaviour of I_c as a function of the applied field, at variance with the simple theoretical scenarios where I_c should just decrease with N_{ext} [1]. The PE is found in our model too (see figure 8), where we can show that it is related to the same kind of phase transition associated with the second peak in the magnetization as we discussed above [6].

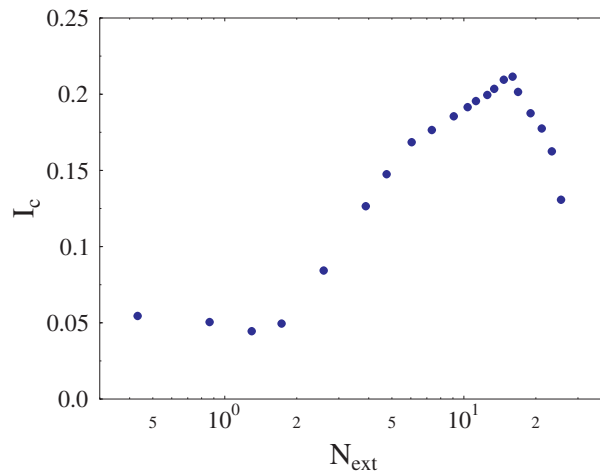


Figure 8. The critical current, I_c , as a function of the applied field, N_{ext} , in the ROM shows a broad peak (called the PE) in corresponding to the location of the ‘second magnetization peak’ (see figure 1).

5. Conclusions

Summarizing, we have shown that a schematic statistical mechanics lattice model [6] for vortices in type-II superconductors (a system of particles diffusing in a pinning landscape) allow us to describe a comprehensive framework of magnetic and transport properties experimentally observed in vortex matter. In particular, here we discussed the interplay between dynamical and equilibrium effects. Interestingly, our results are also supported by some molecular dynamics simulations of more realistic London–Langevin models [16].

We have seen that our model shows a re-entrant melting transition in the field–temperature plane (B, T), analogous to what is observed in vortex matter. At low T , on increasing the field, after the first discontinuous transition and before its re-entrant counterpart, one crosses another first-order phase transition associated with the ‘second magnetization peak’ and with the ‘PE’ observed in the critical current.

The system dynamics exhibits equilibration times which become huge around a crossover point, $T_g(N_{\text{ext}})$, and seem to diverge at a lower temperature, $T_c(N_{\text{ext}})$, where an ‘ideal’ glass transition could be located. Around T_g the system dynamics has a crossover corresponding to a change in microscopic vortex motion: from diffusive (above T_g) to strongly sub-diffusive. Related to that is a crossover from a power law and a Kohlrausch–Williams–Watts law to the logarithmic relaxation found in magnetic creep, which below T_g has apparent ‘aging’ features. The above ‘off-equilibrium’ scenario also explains the experimental finding (previously interpreted in terms of ‘quantum tunnelling’ of vortices [1]) of the existence of a finite creep rate, S_a , when $T \rightarrow 0$. We have briefly outlined the interesting relations with off-equilibrium phenomena in other glass formers such as random magnets and supercooled liquids.

We have also shown that transport properties are strongly related to magnetic creep and we explained a broad set of ‘memory’ effects in vortex flow of driven type II superconductors, such as ‘memory’ and ‘irreversibility’ in I – V characteristics.

Interestingly, a unifying scenario of magnetic and transport properties in vortex physics is beginning to emerge, and the important connections between their equilibrium and off-equilibrium phenomena are becoming clarified.

References

- [1] Blatter G, Feigel'man M V, Geshkenbein V B, Larkin A I and Vinokur V M 1994 *Rev. Mod. Phys.* **66** 1125
 Yeshurun Y, Malozemoff A P and Shaulov A 1996 *Rev. Mod. Phys.* **68** 911
 Brandt E H 1995 *Rep. Prog. Phys.* **58** 1465
 Cohen L F and Jensen H J 1997 *Rep. Prog. Phys.* **60** 1581–672
- [2] Papadopoulos E L, Nordblad P, Svedlindh P, Schöneberger R and Gross R 1999 *Phys. Rev. Lett.* **82** 173
- [3] Banerjee S S *et al* 1999 *Phys. Rev. B* **59** 6043
 Banerjee S S *et al* 2000 *J. Phys. Soc. Japan* **69** 262
 Ling X S *et al* 2001 *Phys. Rev. Lett.* **86** 712
- [4] Henderson W, Andrei E Y, Higgins M J and Bhattacharya S 1996 *Phys. Rev. Lett.* **77** 2077
 Xiao Z L, Andrei E Y and Higgins M J 1999 *Phys. Rev. Lett.* **83** 1664
 Xiao Z L, Andrei E Y, Shuk P and Greenblatt M 2000 *Phys. Rev. Lett.* **85** 3265
- [5] Wen H-h *et al* 1998 *Phys. Rev. Lett.* **80** 3859
 Calame M *et al* 2001 *Phys. Rev. Lett.* **86** 3630
 Sas S *et al* 2000 *Phys. Rev. B* **61** 9118
- [6] Jensen H J and Nicodemi M 2001 *Europhys. Lett.* **54** 566
 Nicodemi M and Jensen H J 2001 *J. Phys. A: Math. Gen.* **34** L11
 Nicodemi M and Jensen H J 2001 *Phys. Rev. Lett.* **86** 4378
 Nicodemi M and Jensen H J 2002 *J. Phys. A: Math. Gen.* **34** 8425
 Jensen H J and Nicodemi M 2002 *Europhys. Lett.* (at press)
 Nicodemi M and Jensen H J 2001 *Phys. Rev. Lett.* **87** 259702
- [7] Ediger M D, Angell C A and Nagel S R 1996 *J. Phys. Chem.* **100** 13 200
 Bouchaud J P, Cugliandolo L F, Kurchan J and Mezard M 1997 *Spin Glasses and Random Fields* ed A P Young (Singapore: World Scientific)
- [8] Daeumling M, Seuntjens J M and Larbaestier D C 1990 *Nature* **346** 332
 Yeshurun Y *et al* 1994 *Phys. Rev. B* **49** 1548
 Perkins G K *et al* 1995 *Phys. Rev. B* **51** 8513
 Ghosh K *et al* 1996 *Phys. Rev. Lett.* **76** 4600
 Khaykovich B *et al* 1996 *Phys. Rev. Lett.* **76** 2555
 Giller D *et al* 1997 *Phys. Rev. Lett.* **79** 2542
 Roy S B and Chaddah P 1997 *J. Phys.: Condens. Matter* **9** L625
 Kokkaliaris S *et al* 1999 *Phys. Rev. Lett.* **82** 5116
 Paltiel Y *et al* 2000 *Nature* **403** 398
 Correa V F, Nieva G and de la Cruz F 1999 *Phys. Rev. Lett.* **83** 5322
- [9] Katz S, Lebowitz J L and Spohn H 1983 *Phys. Rev. B* **28** 1655
 Schmittmann B and Zia R K P 1995 *Phase Transitions and Critical Phenomena* ed C Domb and J L Lebowitz (New York: Academic)
- [10] Mota A C *et al* 1991 *Physica C* **185–9** 343
 Aupke K *et al* 1993 *Physica C* **209** 15
 Hoekstra A F Th 1998 *Phys. Rev. Lett.* **80** 4293
- [11] Fuchs D T *et al* 1998 *Phys. Rev. Lett.* **80** 4971
- [12] Giura M, Marcon R, Silva E and Fastampa R 1992 *Phys. Rev. B* **46** 5753
 Sarti S, Fastampa R, Giura M, Silva E and Marcon R 1995 *Phys. Rev. B* **52** 3734
- [13] Hyman R A, Wallin M, Fisher M P A, Girvin S M and Young A P 1995 *Phys. Rev. B* **51** 15 304
- [14] Lefloch F, Hamman J, Ocio M and Vincent E 1992 *Europhys. Lett.* **18** 647
 Jonason K, Vincent E, Hamman J, Bouchaud J P and Nordblad P 1998 *Phys. Rev. Lett.* **81** 3243
- [15] Bhattacharya S and Higgins M J 1993 *Phys. Rev. Lett.* **70** 2617
 Bhattacharya S and Higgins M J 1995 *Phys. Rev. B* **52** 64
- [16] Jensen H J, Brass A and Berlinsky A J 1988 *Phys. Rev. Lett.* **60** 1676
 Nori F 1996 *Science* **271** 1373
 Kolton A B, Dominguez D and Grönbech-Jensen N 1999 *Phys. Rev. Lett.* **80** 3061
 Reichhardt C, van Otterlo A and Zimanyi G T 2000 *Phys. Rev. Lett.* **84** 1994
 Jackson D K, Nicodemi M, Perkins G, Lindop N A and Jensen H J 2000 *Europhys. Lett.* **52** 210